



# Double-peaked SuperNovae

M. Orellana<sup>1</sup> & M.C. Bersten<sup>2</sup>

<sup>1</sup> *Universidad Nacional de Río Negro. Sede Andina, Argentina*

<sup>2</sup> *Consejo Nacional de Investigaciones Científicas y Técnicas (CONICET), Argentina*

<sup>3</sup> *Instituto de Astrofísica La Plata, CONICET-UNLP, Argentina*

<sup>4</sup> *Facultad de Ciencias Astronómicas y Geofísicas, UNLP, Argentina*

Contact / morellana@unrn.edu.ar

**Resumen** / A través de simulaciones hidrodinámicas 1D, exploramos dos de los escenarios físicos más prometedores invocados para explicar las peculiares supernovas de doble pico. Uno consiste en una doble distribución de níquel radiactivo que se forma cuando parte de este material es expulsado por un supuesto chorro que está relacionado con la explosión de la supernova. El otro escenario solo tiene níquel exterior, pero el pico principal es impulsado por una magnetar recientemente formado. Presentamos toda la evolución de la curva de luz bolométrica para un progenitor rico en helio. El objetivo principal es comparar las curvas de luz bolométricas resultantes y confirmar el hecho de que, para algunos parámetros, los dos picos están claramente separados, siendo este último un pico principal más ancho y brillante.

**Abstract** / Through hydrodynamical 1D simulations we explore two of the more promising physical scenarios invoked to explain peculiar double-peaked supernovae. One consists of a double radioactive nickel distribution formed when some of this material is pushed out by a putative jet that is related to the supernova explosion. The other scenario has only outer nickel, but the main peak is powered by a newly born magnetar. We present the whole evolution of the bolometric light curve for a helium-rich progenitor. The main goal is to compare the resulting bolometric light curves (LCs) and to confirm the fact that, for some parameters, the two peaks are clearly departed, being the latter a brighter and broader main peak.

*Keywords* / stars — supernovae

## 1. Context

We have explored the main competing ideas that were presented in relation to a set of observed double peaked type I SNe that has SN 2005bf (Folatelli et al., 2006) as the archetype case. Only few similar objects were later discovered: PTF11mnb (Taddia et al., 2018) or SN08D Bersten et al. (2013). These SNe share a characteristic rise in luminosity detected prior to the first peak that is produced around 20 days, followed by a main peak at  $\sim 40$  days from the explosion. Such behavior is clearly different from the one modeled as the shock cooling of an extended circumstellar material interaction by Nakar & Piro (2014) where the first peak fades on a timescale of few days after the explosion. For the mentioned sample of SNe, the strongest ideas are related to the presence of radioactive elements, i.e mainly the  $^{56}\text{Ni}$ , at the outer layers of the ejecta (Nishimura et al., 2015). There are many studies in the literature of SNe with outflows or jets (specially in relation to gamma-ray bursts), which motivates the proposal that the jet propagation can induce nucleosynthesis at different layers (Banerjee & Mukhopadhyay, 2013). Therefore we considered two cases:

1. A double nickel distribution that is artificially tuned in this study.
2. Another possibility is the first peak powered by some external nickel and the second one by a central engine. A magnetar as the source that powers the

main peak in SN 2005bf was proposed by Maeda et al. (2007), and explored by using the semianalytic scheme of Kasen & Bildsten (2010). As an improvement, we apply our experience with a hydrodynamic code with the magnetar treated as described in Orellana et al. (2018) and references therein.

## 2. Double nickel profile

To explore both these scenarios, we performed hydrodynamic calculations using different helium rich progenitors. Specifically, we show here models where the pre-SN has  $4 M_{\odot}$  ( $\text{He4}$ ) and its evolution was calculated by Nomoto & Hashimoto (1988) from a main sequence star of  $15 M_{\odot}$ . We have exploded the SNe using the code presented in Bersten et al. (2011), a 1D radiation hydrodynamical code which assumes flux-limited diffusion approximation and gray transfer for the  $\gamma$ -photons produced during the radioactive decay.

In our study the  $^{56}\text{Ni}$  initial profile is modified by tuning the set of parameters indicated in the Fig. 1, with the nickel abundance in departed zones and switch to zero outside that regions or boxes. The extension of the boxes in mass fraction coordinate  $M_r/M$  is determined by the values  $f_0$ ,  $f_1$ ,  $f_2$  and  $f_3$ . The nickel abundance at the inner and outer boxes are named  $X_{\text{in}}$

and  $X_{\text{out}}$ , respectively.

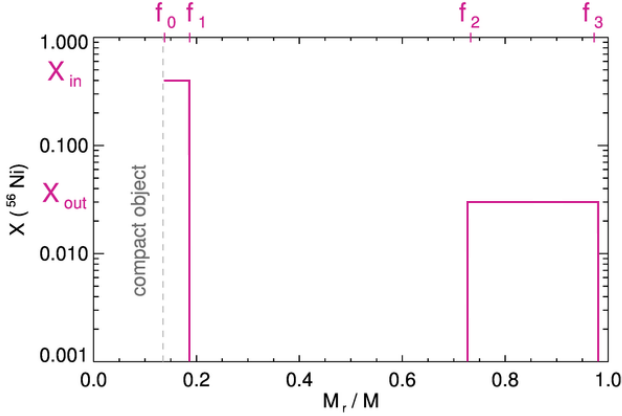


Figure 1: Parameters of a simple profile for the radioactive nickel abundance with two significant zones.

The resulting LCs from the separate changes of the abundances are shown in Fig. 2. We fixed  $f_0 = 0.37$  in order to consider a compact object with mass of a typical neutron star. Also, we set a fixed value of  $f_1$  in each of the other figures of results. The total mass of nickel is limited to be below a typical value of  $\sim 0.1 M_\odot$  in all cases. In Fig. 3 and Fig. 4 we show the impact on the LC of the change into the extension of the outer nickel box. As the other parameters are fixed, the center of the box moves accordingly.

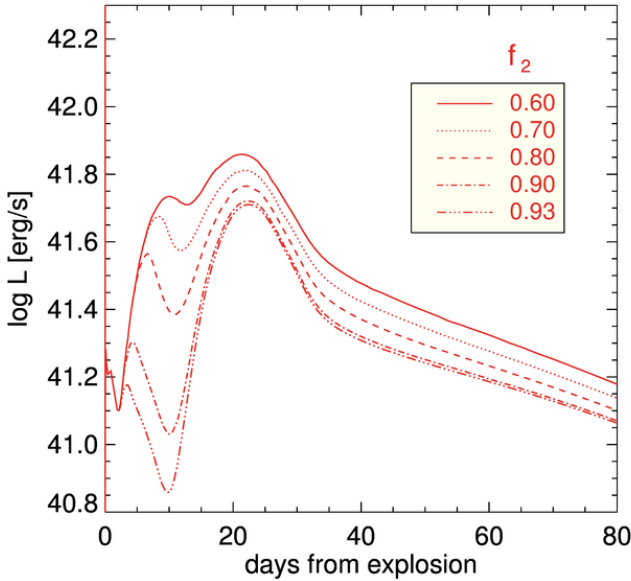


Figure 3: Effect on the LC from variations in the  $f_2$  fraction (inner limit of the outer box) with the other parameters fixed.

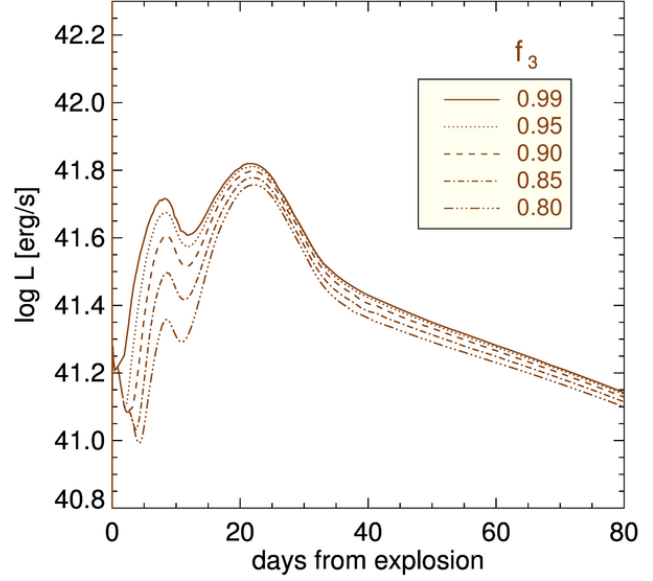


Figure 4: Effect on the LC from variations in the  $f_3$  fraction (outermost limit) with the other parameters fixed.

### 3. Magnetar and outer nickel

The magnetar can be characterized by the initial rotational period,  $P$ , and the magnetic field,  $B$ . In the code, the magnetar is assumed to fully deposit its spin-down energy in the innermost layers of the ejecta. Fig. 5, shows results for the He4 progenitor model with abundance  $X_{\text{out}} = X_{\text{Ni}} \sim 0.01$  for  $f_2 = 0.7$  and  $f_3 = 0.85$  as previously defined, that implies,  $M_{\text{Ni}} = 0.0057 M_\odot$ .

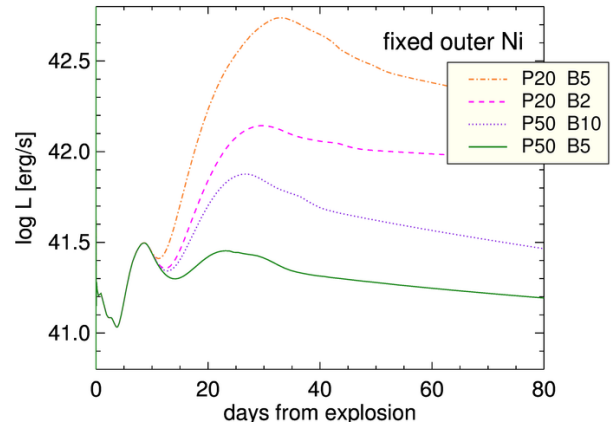


Figure 5: Selected models of magnetars combined with outer  $^{56}\text{Ni}$  that produce two well separated maxima in the LC. The initial period  $P$  is in milliseconds in the legend, and the magnetic field  $B$  in units of  $10^{14}$  G.

Orellana & Bersten (2020) showed a parameter exploration for a hydrogen-poor progenitor with a magnetar. The general trends are here maintained, though in these LCs an initial peak is powered by the nickel. As shown in Fig 5 several possibilities arise from the combined magnetar-nickel power, specially the luminosities

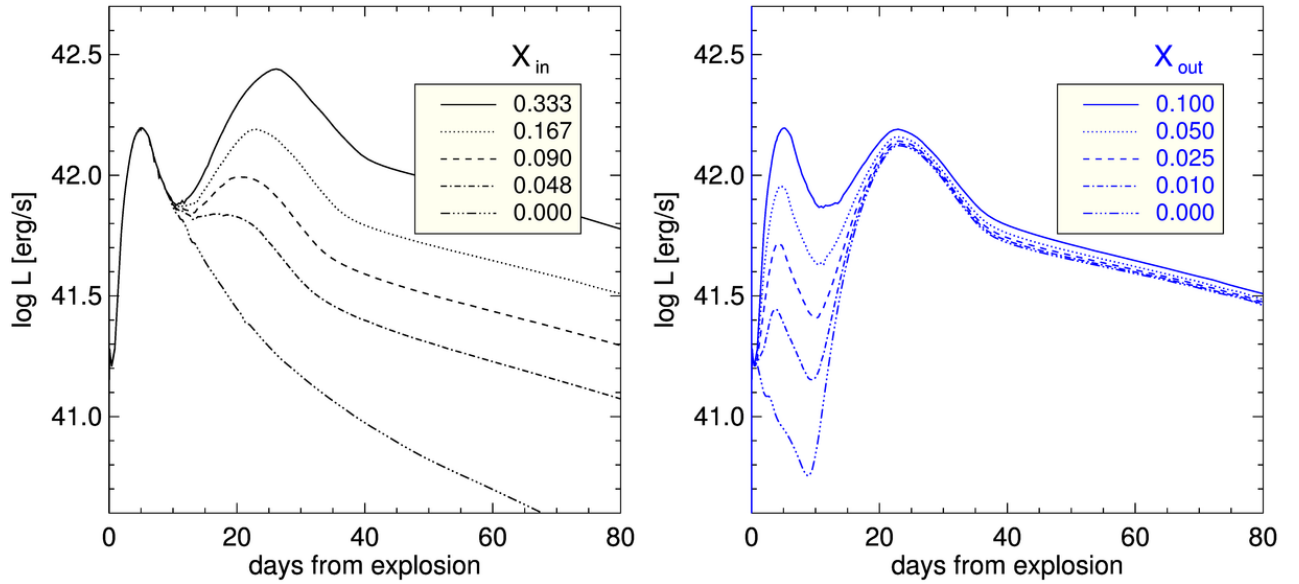


Figure 2: Effect on the LC from variations in the abundance of  $^{56}\text{Ni}$  with the parameters of mass fraction fixed to be  $f_1 = 0.47$ ,  $f_2 = 0.91$ ,  $f_3 = 0.98$ . In the left panel the external box has  $X_{\text{out}} = 0.1$ . In the right  $X_{\text{in}} = 0.2$ .

of the maxima: i.e. when the magnetar is not powerful enough (very large  $P$ , for example) the second peak is dimmer than the first. At the other extreme, a magnetar with  $P$  of a few milliseconds can be so powerful that the first nickel spike is not distinguishable. That can be the case for superluminous supernovae, and needs the inclusion of a relativistic treatment as in Bersten et al. (2016). A time difference between the LC peaks can alternatively be the result of a delay between the initial energy pump of the explosion and the ignition of the magnetar (Dessart et al., 2012).

#### 4. Conclusions

In accordance with other studies our results confirm that a variety of double peaked LCs can be explained by combined nickel and magnetar powering sources. In the case of the double  $^{56}\text{Ni}$  distribution, the parameters fixing the inner  $M_{\text{Ni}}$  determine the luminosity of the second peak, whereas the outer nickel is responsible of the first peak of the light curves.

Adjusting the nickel distribution affects the peaks separation in time and their relative luminosities within certain limitations. Here the effect of  $f_1$  fraction was not included. A systematic and more detailed testing of the double  $^{56}\text{Ni}$  distribution parameter space will be

presented in a forthcoming paper.

*Acknowledgements:* Agradecemos a Claudia Gutiérrez por proponer y discutir con nosotras este tema. Esta investigación es parcialmente financiada por el PI40B696 de la Universidad Nacional de Río Negro, y el PICT-2017-3133.

#### References

- Banerjee I., Mukhopadhyay B., 2013, ApJ, 778, 8
- Bersten M.C., Benvenuto O., Hamuy M., 2011, ApJ, 729, 61
- Bersten M.C., et al., 2013, ApJ, 767, 143
- Bersten M.C., et al., 2016, ApJL, 817, L8
- Dessart L., et al., 2012, MNRAS, 426, L76
- Folatelli G., et al., 2006, ApJ, 641, 1039
- Kasen D., Bildsten L., 2010, ApJ, 717, 245
- Maeda K., et al., 2007, ApJ, 666, 1069
- Nakar E., Piro A.L., 2014, ApJ, 788, 193
- Nishimura N., Takiwaki T., Thielemann F.K., 2015, ApJ, 810, 109
- Nomoto K., Hashimoto M., 1988, Physics Reports, 163, 13
- Orellana M., Bersten M.C., 2020, Boletín de la Asociación Argentina de Astronomía La Plata Argentina, 61B, 63
- Orellana M., Bersten M.C., Moriya T.J., 2018, A&A, 619, A145
- Taddia F., et al., 2018, A&A, 609, A106